

Single-electron switching in $\text{Al}_x\text{Ga}_{1-x}\text{As}/\text{GaAs}$ Hall devices

著者	Muller Jens, Li Yongqing, Molnar Stephan von, Ohno Yuzo, Ohno Hideo
journal or publication title	Physical Review. B
volume	74
number	12
page range	125310
year	2006
URL	http://hdl.handle.net/10097/53522

doi: 10.1103/PhysRevB.74.125310

Single-electron switching in $\text{Al}_x\text{Ga}_{1-x}\text{As}/\text{GaAs}$ Hall devices

Jens Müller,* Yongqing Li,[†] and Stephan von Molnár

Center for Materials Research and Technology (MARTECH), Florida State University, Tallahassee, Florida 32306-4351, USA

Yuzo Ohno and Hideo Ohno

Laboratory for Nanoelectronics and Spintronics, Research Institute for Electrical Communication, Tohoku University, Sendai, Japan

(Received 9 December 2005; revised manuscript received 25 July 2006; published 15 September 2006)

We report on measurements of low-frequency noise in submicron Hall devices based on $\text{Al}_x\text{Ga}_{1-x}\text{As}/\text{GaAs}$ heterostructures. In addition to the $1/f$ -type noise caused by switching events in the n - AlGaAs layer we observe a random telegraph signal in the time domain at elevated temperatures which we attribute to trapping or detrapping of a single electron from a deep donor (DX -type) center located near the space charge region in the vicinity of the $\text{Al}_x\text{Ga}_{1-x}\text{As}/\text{GaAs}$ interface. A simple two-level model accounts for the observed gate-voltage dependence of the electronic transition rates.

DOI: [10.1103/PhysRevB.74.125310](https://doi.org/10.1103/PhysRevB.74.125310)

PACS number(s): 85.30.-z, 73.23.-b, 74.40.+k

I. INTRODUCTION

A. $\text{Al}_x\text{Ga}_{1-x}\text{As}/\text{GaAs}$ Hall devices

Two-dimensional electron systems (2DES) in III/V semiconductor heterostructures such as n - $\text{Al}_x\text{Ga}_{1-x}\text{As}/\text{GaAs}$ grown by molecular beam epitaxy are the subjects of continuing interest in both fundamental investigations and electronic-device applications, as e.g., the integer and fractional quantum Hall effect, the implementation of solid-state quantum bits, high-speed modulation-doped field effect transistors, or high-sensitivity Hall magnetometers. The 2DES is formed at the heterointerface of the n - $\text{Al}_x\text{Ga}_{1-x}\text{As}/\text{GaAs}$ layer where, due to band alignment, an approximately triangular potential well forms. The particularly high-electron mobility in these materials is achieved by inserting an undoped $\text{Al}_x\text{Ga}_{1-x}\text{As}$ spacer layer between the Si-doped n - $\text{Al}_x\text{Ga}_{1-x}\text{As}$ and the smaller band-gap material GaAs which physically separates the carriers from their parent donor atoms and thereby reduces the scattering off these ionized impurities.

Besides applications in electronic circuits, high-mobility materials are suitable for making high-sensitivity Hall devices. Indeed, Hall devices based on 2DES semiconductor heterostructures are of increasing interest as noninvasive high-sensitivity magnetometers for nanoscale magnetic measurements and biological sensing (see, e.g., Refs. 1–3 and references therein). We recently presented two noise studies, aiming at a systematic characterization of low-frequency fluctuations in micron and submicron Hall devices.^{4,5} In Ref. 4 a surprisingly large gating effect on the $1/f$ noise is discussed; the noise level can be suppressed by more than two orders of magnitude with a moderate positive gate voltage of 200 mV, whereas the carrier density is only increased by about 60% in the same interval. It was concluded that the $1/f$ noise originates from remote switching processes in the highly doped n - AlGaAs layer, which are only weakly coupled to the 2DES, e.g., by affecting the mobility of the free carriers. The strong temperature dependence of the noise spectra at intermediate-gate voltages made it possible to extract the corresponding activation energies based on thermally activated processes and the Dutta-Dimon-Horn

model.⁶ The observed gate-voltage dependence of the noise can then be explained by changes in the activation-energy distribution, which varies as the applied gate voltage modifies band bending of the 2DES heterostructure.⁴ For magnetic measurements, a moment sensitivity better than $10^4 \mu_B/\text{Hz}^{1/2}$ at 1 Hz has been achieved at $T=15$ K in a perpendicular background field of $B=0.25$ T. These results have been reproduced by noise studies in similar devices made from different wafer material⁵ which established the universality of this large gating effect on the $1/f$ noise for the present $\text{Al}_x\text{Ga}_{1-x}\text{As}/\text{GaAs}$ heterostructures. In Ref. 5 the $1/f$ noise has been studied systematically as a function of the width of the conducting channel. In a sample as small as $0.45 \mu\text{m}$ we observe a nonmonotonic temperature dependence of the low-frequency noise power spectral densities (PSD) and deviations from $1/f$ -type behavior to a thermally activated Lorentzian-type PSD. The Lorentzian is described by a two-rate kinetics and a single activation energy and attempt rate. Hence, in small-area Hall devices a systematic decomposition of the $1/f$ noise in the Hall voltage to its Lorentzian constituents, and thus, the kinetic signature of a single fluctuator in the noise spectrum is observed.⁵

Noise studies like the present one provide direct information about the ultimate limits of low-frequency applications in certain device structures. Furthermore, intrinsic fluctuations are fingerprints of the internal dynamics. Besides the information about intrinsic conductivity properties, such as the microscopic behavior of charge carriers and their coupling to lattice defects, electronic traps, and magnetic moments, it is worth noting that noise in semiconductor devices is not always unwelcome. Random telegraph noise related to paramagnetic defects near the Si/SiO₂ interface in a MOSFET-type structure has recently been utilized to detect spin resonance of a single electron.^{24,25}

B. Mechanisms of noise in $\text{Al}_x\text{Ga}_{1-x}\text{As}/\text{GaAs}$ -based structures

Since the invention of $\text{Al}_x\text{Ga}_{1-x}\text{As}/\text{GaAs}$ heterostructures⁷ there is a long history of noise studies of the field-effect transistor (FET), the quantum point contact (QPC), and Hall-bar structures (see, e.g., Refs. 8–23). In these stud-

ies different mechanisms of the noise have been suggested, as discussed below. A complex interplay of these mechanisms may determine the noise behavior in relatively large samples of GaAs-based materials, whereas in smaller devices the origin of a particular noise pattern may be identified. A crucial point in all of these investigations is that usually fluctuations in the resistance and/or Hall voltage of the 2DES in $\text{Al}_x\text{Ga}_{1-x}\text{As}/\text{GaAs}$ heterostructures are measured, whereas the origin of the noise is related to the (bulk) $\text{Al}_x\text{Ga}_{1-x}\text{As}$ layer which is separated by a potential barrier from the 2DES. Thus, in order to understand the origin of the noise, the coupling of the 2DES to fluctuations in the remote n -doped $\text{Al}_x\text{Ga}_{1-x}\text{As}$ layer or close to the interface has to be addressed. For example, trapping and detrapping events of electrons in n - $\text{Al}_x\text{Ga}_{1-x}\text{As}$, i.e., changes in the charge states of so-called DX centers, will affect the conduction in the 2DES by a combination of electron mobility and density fluctuations, as has been pointed out by Kirtley *et al.*⁹ Similar results on gated and ungated structures have been reported in Refs. 8, 10, 11, 14, 16, 18–20, and 22. Electron trapping as the origin of noise has also been discussed in quantum point contacts,^{13,15,17,26} where discrete fluctuations in the channel conductance have been observed. Different explanations for the noise behavior are related to the issue noted above, namely, how the switching events couple to the electron system whose noise is actually measured.

The above selected examples of earlier noise studies in $\text{AlGaAs}/\text{GaAs}$ -based structures show that a special kind of trap, the DX center, plays an important role for the transport properties of these structures. The DX center is a distorted state of isolated donors showing such interesting features as large lattice relaxation, strong electron-phonon coupling, the existence of metastable excited states giving rise to persistent photoconductivity, and a negative- U many-body effect.^{27–29} The DX center is the result of a so-called “shallow-to-deep transformation” of substitutional donors in GaAs induced by changes in the conduction band structure; the latter can be achieved either by changing the alloy composition or applying hydrostatic pressure. The trap level associated with the DX center in $\text{Al}_x\text{Ga}_{1-x}\text{As}$ approximately follows the L -band edge and for $x > 0.22$ the DX state is the lowest-lying donor state and controls the conductivity of the material.^{28,29} It is formed by one neutral donor capturing an electron from another neutral donor atom according to $2d^0 \rightarrow d^+ + DX^-$. The resultant DX center is negatively charged and contains two electrons localized on the same donor atom which attract each other as a result of electron-lattice interaction. The DX^- defect formation involves a large bond-rupturing displacement of either the defect atom or the host lattice atoms. Such a deep and localized state becomes stable because of the near degeneracy between the three conduction minima Γ , L , and X which energetically favors the electron wave function to be delocalized in reciprocal space while localizing in real space. This localization is achieved via a large lattice distortion.³⁰

In the present paper we report measurements on a submicron $\text{AlGaAs}/\text{GaAs}$ Hall bar structure (feature size $w \sim 0.7 \mu\text{m}$). While the measured PSD are of $1/f$ -type in a wide temperature range from 4.2–100 K, additional random telegraph noise in the time domain occurs at elevated temperatures around 70 K which we attribute to single electron

trapping/detrapping from a deep donor state close to the $\text{Al}_x\text{Ga}_{1-x}\text{As}/\text{GaAs}$ interface into the conduction band. In agreement with a simple model, we find that applying a gate voltage strongly modifies the energy barrier of the thermally activated electron-capture process. The measurements presented here extend earlier studies of resistance fluctuations in $\text{Al}_x\text{Ga}_{1-x}\text{As}/\text{GaAs}$ FET's and QPC's and Hall-voltage fluctuations in relatively large structures to a new parameter range and—besides providing valuable information about the limiting factors for low-frequency device performance—may increase our understanding of the dynamic aspects of transport properties in these materials as single-fluctuator noise provides a unique method to probe the underlying physical mechanism for the fluctuations.

II. EXPERIMENT AND SAMPLE CHARACTERIZATION

The $\text{Al}_x\text{Ga}_{1-x}\text{As}/\text{GaAs}$ heterostructure used in this study was grown on an undoped semi-insulating GaAs (100) substrate and AlAs/GaAs superlattice buffer layer, and consists of a 1000-nm-thick undoped GaAs layer, a 30-nm-thick undoped $\text{Al}_{0.29}\text{Ga}_{0.71}\text{As}$ spacer layer, and a 100-nm-thick Si-doped $\text{Al}_{0.29}\text{Ga}_{0.71}\text{As}$ layer with a dopant density of $1 \times 10^{18} \text{ cm}^{-3}$ and a 10-nm-thick GaAs cap layer. The electron density and Hall mobility of submicron structures patterned from these wafers were determined in the Hall-effect measurements to be $n \sim 1.2 \times 10^{11} \text{ cm}^{-2}$ and $\mu_H \sim 1 \times 10^5 \text{ cm}^2/\text{V s}$ in the dark, and at low temperatures and zero gate voltage. Application of a positive gate voltage $V_g = 200 \text{ mV}$ increases the carrier concentration to $n \sim 1.8 \times 10^{11} \text{ cm}^{-2}$. A submicron Hall-bar pattern of feature size $w \sim 0.7 \mu\text{m}$ was fabricated by electron-beam lithography followed by wet chemical etching.³¹ A 50-nm-thick Cr/Au gate was deposited on top of the structure. Electrical contacts made by alloying In/Sn are Ohmic. The present device is the same as the one used for the detailed studies of the $1/f$ noise characteristics and its gate-voltage dependence reported in Ref. 4. The data on this sample are representative since similar random telegraph noise has been observed on other submicron-size samples fabricated from the same and also from other wafers. The random telegraph switching under study has been reproducibly observed in various cool downs.

The noise-power spectral density of the Hall voltage was measured using a seven-terminal ac gradiometry setup where two currents I_1 and I_2 are applied with opposite directions to two Hall crosses. The electronic circuit allows balancing both amplitude and phase of the currents, so that the Hall gradiometer output ΔV_H has zero offset. Details of this technique are described elsewhere.^{4,32} The real-time measurements of the Hall voltage were performed using standard lock-in techniques. Care was taken that all spurious sources of noise, especially those coming from the gate itself could be ruled out or eliminated.

Technically, Ohmic contacts to the 2DES are also contacting the flat-band region of the (low-mobility) $\text{Al}_x\text{Ga}_{1-x}\text{As}$ layer, which is thus always measured in parallel. The carrier density n in the $\text{Al}_x\text{Ga}_{1-x}\text{As}$ region is governed by deep donor (DX) levels. For $x > 0.22$ the energy level E_{DX} lies well below the band edge,^{28,29} and even at room temperature

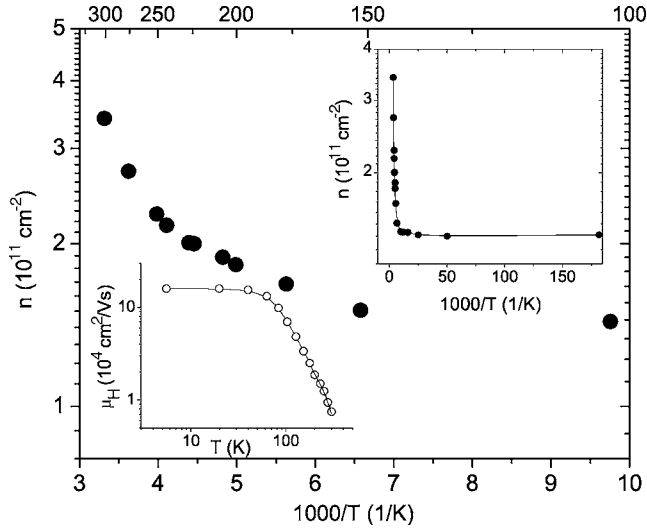


FIG. 1. Carrier concentration of a relatively large sample (5×10) μm^2 , fabricated from the same wafer as the submicron sample discussed below, as determined from the Hall-effect measurements as a function of reciprocal temperature from room temperature down to 100 K. The upper right inset shows the temperature range down to 4.2 K. Lower left inset, Hall mobility as a function of temperature. Lines are guides to the eye.

many carriers are frozen out to the trap level. Thus, as $n_{\text{Al}_x\text{Ga}_{1-x}\text{As}}$ decreases exponentially with $1/T$, parallel conduction in the $n\text{-Al}_x\text{Ga}_{1-x}\text{As}$ layer is negligible. This is confirmed by Hall-effect measurements of the carrier concentration (see Fig. 1). Below about 100 K (where all the measurements presented in this paper were performed) the carrier concentration of the device is essentially constant (see the upper inset of Fig. 1), which means that the conduction is completely determined by the 2DES in agreement with earlier observations.^{9,11,16} The lower inset of Fig. 1 shows the temperature dependence of the Hall mobility which agrees well with remote impurity scattering as the limiting factor at low temperatures.³³

In the configuration coordinate diagram after Mooney^{28,29} the DX center is characterized by the donor binding energy E_d , the optical ionization energy E_o , the activation energy for emission of an electron from the DX level to the conduction band E_e , and the activation energy for the capture of an electron from the conduction band E_c ; the latter two of which are determined from the kinetics of electron transitions.²⁸ E_d is the energy position of the DX level with respect to the bottom of the conduction band and can be determined from Hall-effect measurements. Using the parallel layer method³⁴ and assuming that the 2DES is also dominant at room temperature gives $n_H = n_{2\text{DES}} + 2n_{\text{Al}_x\text{Ga}_{1-x}\text{As}}(\mu_{\text{Al}_x\text{Ga}_{1-x}\text{As}}/\mu_{2\text{DES}})$,^{11,16} where n_H denotes the measured Hall carrier concentrations $n_{2\text{DES}}$ and n_{AlGaAs} , the carrier concentration in the 2DES and the flat-band region of $n\text{-Al}_x\text{Ga}_{1-x}\text{As}$, respectively, and $\mu_{2\text{DES}}$ and $\mu_{\text{Al}_x\text{Ga}_{1-x}\text{As}}$, the corresponding Hall mobilities. Using $n_{\text{Al}_x\text{Ga}_{1-x}\text{As}} \propto \exp(-E_d/k_B T)$ we find from the high-temperature data in Fig. 1, a value of $E_d \sim 41$ meV which agrees reasonably well with 49 meV as expected for x

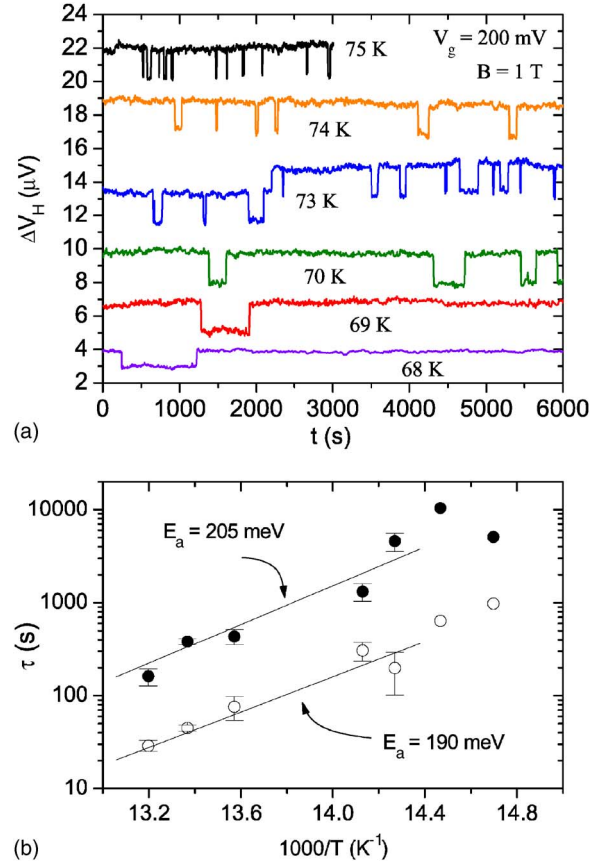


FIG. 2. (Color online) (a) Hall voltage ΔV_H against time taken at different temperatures and $V_g = 200$ mV, $B = 1$ T, and $I = 2$ μA . Curves are shifted for clarity. (b) Average lifetimes of the higher and lower Hall-voltage states plotted versus the reciprocal temperature. Lines are linear fits according to Eq. (1). Error bars denote the statistical standard error. For the temperatures represented by points without error bars, only limited statistics are available; these points have not been included in the fit.

$= 0.29$, by assuming that the thermal depth of the DX center is found to vary almost linearly from 0 to 160 meV with x from 0.22 to 0.45 (see Ref. 28).

III. RESULTS AND DISCUSSION

Figure 2 shows the measured Hall voltage ΔV_H as a function of time for different temperatures 68–75 K taken at a fixed gate voltage of $V_g = 200$ mV. At this gate voltage the level of $1/f$ noise is substantially suppressed [see Fig. 3(b)]. The data clearly show switching between two distinct states of higher and lower Hall voltages, states “high” and “low,” respectively. At all temperatures, the systems spend more time in state high whereas the average lifetimes of both states become shorter with increasing temperature.³⁵ The curve taken at 73 K in Fig. 2(a) shows another switching event of same amplitude, i.e., apparently there are three distinct states instead of only two. However, in the following analysis we will consider only a two-level system which is justified for the following reasons: (i) the time scale of the additional (reversible) switching events is found to be in the order of

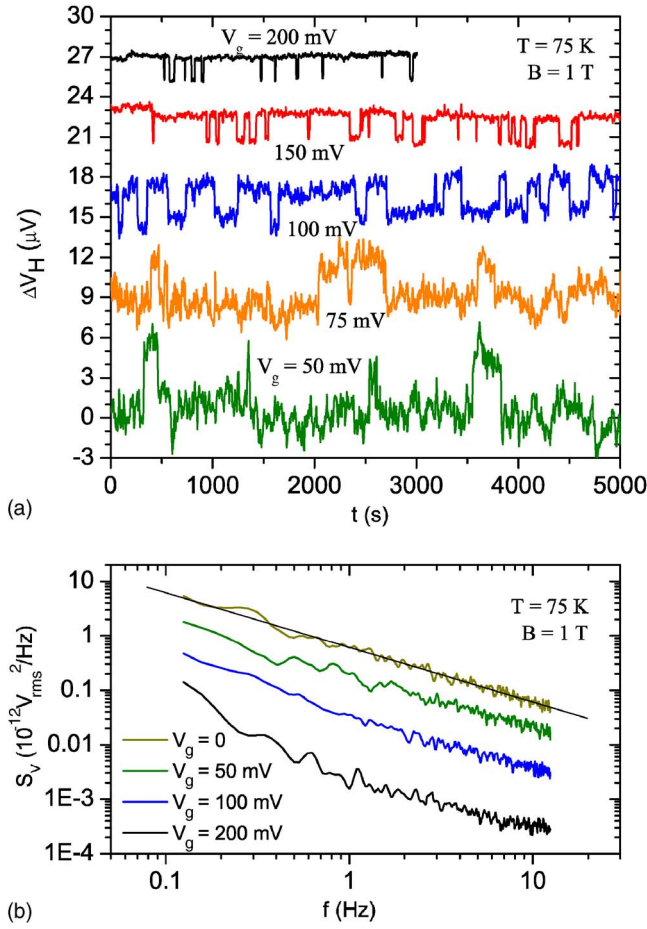


FIG. 3. (Color online) (a) Hall voltage ΔV_H against time taken at different gate voltages and $T=75\text{ K}$, $B=1\text{ T}$, and $I=2\ \mu\text{A}$. Curves are shifted for clarity. (b) Corresponding noise power spectral densities (PSD) at different gate voltages, showing the large suppression of the noise level with gating, see also Ref. 4. The straight line is a fit to the data at zero gate voltage to $S_V \propto 1/f^\alpha$ yielding $\alpha=1$.

10^4 s and thus at least one order of magnitude greater than those of the shorter two-level switching events, and (ii) the average lifetimes of the shorter-lived two-level system have been found to be independent of the actual state related to the much longer lifetime. Thus, these are independent switching events which can be analyzed separately.

Considering the simple case of a two-level system, i.e., a double-well model with thermally activated switching between two states, the average time τ_i spent in state i can be described by an Arrhenius law

$$\tau_i = \nu_{0,i}^{-1} \exp(E_{a,i}/k_B T), \quad (1)$$

where $E_{a,i}$ is the barrier height to escape from state i , k_B is the Boltzmann constant, and $\nu_{0,i}$ an attempt frequency. We find that the distribution of transition times is close to a Poisson distribution which shows that the transitions from one state to another occur randomly. Figure 2(b) shows the average lifetimes $\langle \tau_i \rangle$ (later identified as τ_c and τ_e) in an Arrhenius plot. Although limited in temperature range,³⁶ fits to Eq. (1) give an estimate of the activation energies of E_a

$= (205 \pm 40)\text{ meV}$ and $(190 \pm 40)\text{ meV}$ for the higher and lower Hall voltage state, respectively, and attempt frequencies of the order of $\nu_0 \sim 2 \times 10^{11}\text{ Hz}$.³⁷ These values for the activation energies are within the range (however, at the lower end) of capture and emission energies reported in the extensive literature; see e.g., Refs. 9–11, 16, 19, 28, and 38.

Values for the activation energies in the order of 200 meV are significantly larger than the values of $E_a \sim 24$ and 12 meV which have been deduced from the Dutta-Dimon-Horn model in the same sample at $T=22\text{--}35\text{ K}$ ($V_g=75\text{ mV}$) and $T=21\text{--}45\text{ K}$ ($V_g=100\text{ mV}$), respectively, and $E_a=88\text{ meV}$ at $T=43\text{--}53\text{ K}$ ($V_g=200\text{ mV}$, different sample) for the thermally activated switching processes in the remote impurity layer which are responsible for the $1/f$ noise.^{4,5} Also, for the latter type of noise, attempt frequencies in the order of 10^9 Hz have been found. These deviations suggest that the origin of the random telegraph signal (RTS) observed at elevated temperatures around 70 K is different from that which causes the $1/f$ -type noise spectra.

Discrete switching which depends on the gate voltage (see Fig. 3 and discussion below) implicates individual fluctuators and electron trapping. Thus, it appears natural to identify the average lifetimes $\langle \tau_i \rangle$ of the higher and lower Hall voltage states with emission and capture times τ_e and τ_c , respectively. It has been pointed out by Kurdak *et al.*²⁰ that if a typical switching event is electron trapping, it would modulate the number of carriers by 1. On the other hand, a remote event which is weakly coupled to the 2DES has less impact on the carriers in the sample and therefore, would modulate the total number of electrons by much less than 1. Assuming that Hall voltage fluctuations are affected by carrier density fluctuations only, the relative change in the measured Hall voltage is given by $\Delta V_H/V_H = -\Delta n/n = -\Delta N/N$, where $N = nA$ denotes the total number of carriers and A the active area of the Hall cross. Because we observe mainly a two-state RTS, the change in $\Delta V_H = V_{H1} - V_{H2}$ is caused by fluctuations in one of the Hall crosses instead of two. Using $\Delta V_H \sim 2\ \mu\text{V}$ as read from Fig. 2(a) we estimate $\Delta V_H/V_H = -\Delta N/N \approx 1/3000$ with $N \approx 900$, leading to $\Delta N \sim 0.3 \pm 0.1$ which is less than unity. Possibly the switching event also affects the mobility of the channel.

The amplitude of the switching event, which is less (but not much less) than unity, as well as the relative large value of the activation energy, suggest that changes in the charge state of a DX -type trap in the region of band bending near the $\text{Al}_x\text{Ga}_{1-x}\text{As}/\text{GaAs}$ interface cause the observed discrete fluctuations in the Hall voltage, in contrast to a switching event in the remote $n\text{-Al}_x\text{Ga}_{1-x}\text{As}$ layer. A better understanding of the switching kinetics might come from investigations of the gate voltage dependence on the noise. Figure 3(a) shows time traces of the Hall voltage taken at a fixed temperature of 75 K and different gate voltages. For comparison, Fig. 3(b) shows the low-frequency noise power spectral densities of the Hall voltage taken at the same conditions. The PSD in the present frequency range show a purely $1/f$ -type behavior. Also—as for the temperature range between 1.5 K and 60 K⁴—the noise level at 75 K is largely suppressed by applying moderate gate voltages (e.g., at 1 Hz by a factor of ~ 400 for $V_g=200\text{ mV}$). The fact that the PSD stays $1/f$ -like

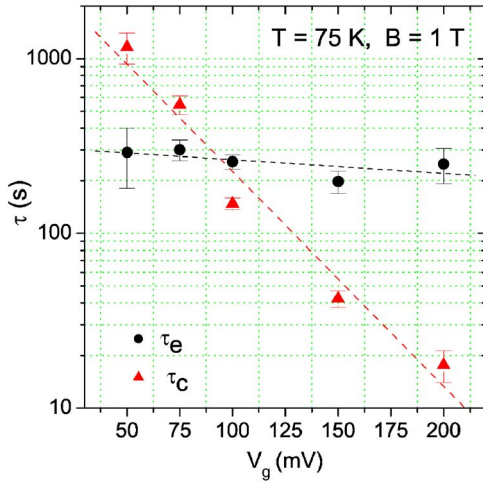


FIG. 4. (Color online) Average lifetimes of the higher and lower Hall-voltage states plotted versus gate voltage. Error bars denote the statistical standard error. Lines are guides to the eye.

while for the same parameters a RTS is measured in the time domain corroborates that these two kinds of noise originate from different mechanisms; obviously the amplitude of the Lorentzian-type spectrum which belongs to the RTS is too small to be observed in the present frequency range.

As seen in Fig. 3(a), the effect of changing the gate voltage on the Hall voltage signal ΔV_H is twofold. First, according to the PSD shown in Fig. 3(b), decreasing the gate voltage V_g increases the overall $1/f$ -type noise; the time traces $\Delta V_H(t)$ become noisier for smaller values of V_g . Second, there is a striking change in the random telegraph signal; with decreasing gate voltage the ratio of the average lifetimes of the higher and lower Hall voltage states reverses. Whereas at higher values of V_g the system spends more time in the high state, the low state becomes more stable at lower gate voltages. Figure 4 shows the average lifetimes of the electronic states as a function of gate voltage with an apparent crossover around $V_g \sim 90$ mV.³⁹ The applied gate voltage obviously strongly alters the shape of the double-well potential of the two-level system. Remarkably, the average lifetime of state high (i.e., higher Hall voltage at large gate voltages) is only very weakly dependent on the gate voltage, whereas state low shows a strong gate-voltage dependence. This behavior can be explained by considering a deep trap located in the vicinity of the GaAs/ $\text{Al}_x\text{Ga}_{1-x}\text{As}$ interface with energy level E_T which is separated by a repulsive energy barrier from the conduction band energy E_C . A calculation of the conduction band offset⁴⁰ gives $E_c = 253.3$ meV for the present structure with $x = 0.29$ at $T = 77$ K and for the Fermi level $E_F = 38.7$ meV (measured from the conduction band) at the interface, and therefore, a barrier height of about 210–215 meV in good agreement with the values for the activation energy found in our measurements. This supports the assumption of the switching process taking place close to the interface. We further assume that the trap level only interacts with the conduction band. If the transition to and from the trap occurs via intermediate short-lived (L -band) states, the capture rate for the empty trap involves the sum of the activation energies for multiphonon capture and for the

population of the intermediate state.^{9,28} According to this model, the capture rate would strongly depend on the applied gate voltage as changes in V_g essentially shift the quasi-Fermi level (which is almost flat at the heterointerface side, see Ref. 41) whereas the emission rate, which only depends on the depth of the trap level, would not be affected by V_g . This simple model indeed accounts for the observations shown in Fig. 4 and allows for an identification of the formerly labeled high and low states with filled and empty trap states, respectively.

For individual RTS generated by a trap with energy level E_T and mean capture and emission times τ_c and τ_e , respectively, one has from detailed balance,

$$\frac{\tau_c}{\tau_e} = g \exp \frac{E_T - E_F}{k_B T}, \quad (2)$$

where g is the degeneracy factor and E_F the Fermi energy. Following the analysis of RTS in Si-MOSFET structures given in Refs. 42 and 43, the change of the Fermi energy relative to the trap energy level with applied gate voltage may be related to the measured gate-voltage dependencies of the capture and emission times,

$$\frac{d(E_T - E_F)}{dV_g} = k_B T \frac{d(\ln \tau_c - \ln \tau_e)}{dV_g}. \quad (3)$$

From Fig. 4 we read $d(E_T - E_F)/dV_g = -(170 \pm 15)$ meV/V. In the present case, the quasi-Fermi level lies below the trap level at zero and small gate voltages. Upon increasing gate voltages, E_F then crosses E_T at around $V_g \sim 90$ meV where the average capture and emission times are equal. At larger gate voltages, the Fermi level lies above the trap energy level. In the region of band bending, where we assume that the generation process takes place, the distance between the Fermi level and the conduction band at a given gate voltage is not constant, and the capture and emission rates are spatially dependent. A rough estimate yields $d \sim 4$ nm for the distance of the trap from the interface (cf. Refs. 10, 24, 42, and 43).

In the above model the capture and/or emission of an electron from the trap into the conduction band changes the charge state of a DX center which causes local fluctuations in the electron density and/or the change in the Coulomb potential modulates the conductance of the 2DES. In contrast, a direct transition of an electron across the $\text{Al}_x\text{Ga}_{1-x}\text{As}/\text{GaAs}$ interface where the electron which is generated into the conduction band will be scattered into the conducting channel, and thus increase the number of carriers in the system by one, has been suggested in Refs. 10, 11, and 16, based on noise spectroscopy in similar structures to the one investigated here. Also, direct tunneling from electronic surface states might be considered. However, the above estimate of a change in the absolute carrier number less than unity and the estimated distance of the trap from the interface suggest a more weakly coupled mechanism in the present case. Since in Refs. 10, 11, and 16 extremely broadened Lorentzian-type PSD, i.e., ensembles of fluctuators, have been analyzed, the present data give direct evidence for an individual carrier generation process in the vicinity of the space charge region

at the $\text{Al}_x\text{Ga}_{1-x}\text{As}/\text{GaAs}$ interface. In future experiments the field dependence of the transition kinetics may provide valuable information about the magnetic degrees of freedom of the switching electron (see Refs. 24 and 25).

IV. SUMMARY

We performed noise studies on a submicron Hall device made from gated $\text{Al}_x\text{Ga}_{1-x}\text{As}/\text{GaAs}$ heterostructures. In submicron-size samples we find additional, random telegraph-type noise at elevated temperatures, which we interpret as trapping or detrapping events of a single electron. We considered a simple two-level model of emission from a deep donor (DX center) state located in the region of band bending at the $\text{Al}_x\text{Ga}_{1-x}\text{As}/\text{GaAs}$ interface into the conduc-

tion band. There, the change of the DX center's charge state causes fluctuations of the local electron density and/or modulates the conductance of the channel. The model accounts for the observed gate voltage dependence of the transition rates and the energy of the identified trap level with respect to the Fermi energy.

ACKNOWLEDGMENTS

We gratefully acknowledge fruitful discussions with Peng Xiong. Work supported by NSF Grant No. DMR0072395 and DARPA through ONR Grants No. N-00014-99-1-1094 and No. MDA-972-02-1-0002. The work at Tohoku University was supported partially by a Grant-in-Aid from the Ministry of Education, Japan.

*Present address: Max-Planck-Institut für Chemische Physik fester Stoffe, D-01187 Dresden, Germany. Electronic address: mueller@cpfs.mpg.de

†Present address: Max-Planck-Institut für Festkörperforschung, D-70569 Stuttgart, Germany.

¹Y. Li, P. Xiong, S. von Molnár, S. Wirth, Y. Ohno, and H. Ohno, *Appl. Phys. Lett.* **80**, 4644 (2002).

²K. Novoselov, S. Morozov, S. Dubonos, M. Missous, A. Volkov, D. Christian, and A. Geim, *J. Appl. Phys.* **93**, 10053 (2003).

³G. Mihajlović, P. Xiong, S. von Molnár, K. Ohtani, H. Ohno, M. Field, and G. Sullivan, *Appl. Phys. Lett.* **87**, 112502 (2005).

⁴Y. Li, C. Ren, P. Xiong, S. von Molnár, Y. Ohno, and H. Ohno, *Phys. Rev. Lett.* **93**, 246602 (2004).

⁵J. Müller, S. von Molnár, Y. Ohno, and H. Ohno, *Phys. Rev. Lett.* **96**, 186601 (2006).

⁶P. Dutta, P. Dimon, and P. M. Horn, *Phys. Rev. Lett.* **43**, 646 (1979).

⁷H. Störmer, R. Dingle, A. Gossard, W. Wiegmann, and M. Sturge, *Solid State Commun.* **29**, 705 (1979).

⁸S.-H. J. Liu, M. Das, C. Peng, J. Klem, T. Henderson, W. Kopp, and H. Morkoç, *IEEE Electron Device Lett.* **6**, 453 (1985).

⁹J. Kirtley, T. Theis, P. Mooney, and S. Wright, *J. Appl. Phys.* **63**, 1541 (1988).

¹⁰S. Kugler, *J. Appl. Phys.* **66**, 219 (1989).

¹¹F. Hofman, R. Zijlstra, and J. Defreitas, *J. Appl. Phys.* **67**, 2482 (1990).

¹²J. Peransin, P. Vignaud, D. Rigaud, and L. Vandamme, *IEEE Trans. Electron Devices* **37**, 2250 (1990).

¹³C. Dekker, A. J. Scholten, F. Liefrink, R. Eppenga, H. van Houten, and C. T. Foxon, *Phys. Rev. Lett.* **66**, 2148 (1991).

¹⁴S. Tehrani, A. van Rheenen, M. Hoogstra, J. Curless, and M. Peffley, *IEEE Trans. Electron Devices* **39**, 1070 (1992).

¹⁵D. H. Cobden, A. Savchenko, M. Pepper, N. K. Patel, D. A. Ritchie, J. E. F. Frost, and G. A. C. Jones, *Phys. Rev. Lett.* **69**, 502 (1992).

¹⁶L. Ren and M. Leys, *Physica B* **192**, 303 (1993).

¹⁷T. Sakamoto, Y. Nakamura, and K. Nakamura, *Appl. Phys. Lett.* **67**, 2220 (1995).

¹⁸M. Py and H.-J. Buehlmann, *J. Appl. Phys.* **80**, 1583 (1996).

¹⁹D. D. Carey, S. T. Stoddart, S. J. Bending, J. J. Harris, and C. T.

Foxon, *Phys. Rev. B* **54**, 2813 (1996).

²⁰Ç. Kurdak, C.-J. Chen, D. C. Tsui, S. Parihar, S. Lyon, and G. W. Weimann, *Phys. Rev. B* **56**, 9813 (1997).

²¹M. Pioro-Ladrière, J. H. Davies, A. R. Long, A. S. Sachrajda, L. Gaudreau, P. Zawadzki, J. Lapointe, J. Gupta, Z. Wasilewski, and S. Studenikin, *Phys. Rev. B* **72**, 115331 (2005).

²²R. Khilil, A. El Hdiy, and Y. Jin, *J. Appl. Phys.* **98**, 093709 (2005).

²³V. P. Kunets, R. Pomraenke, J. Dobbert, H. Kissel, U. Müller, H. Kostial, E. Wiebicke, G. G. Tarasov, Y. I. Mazur, and W. T. Masselink, *IEEE Sens. J.* **5**, 883 (2005).

²⁴M. Xiao, I. Martin, and H. W. Jiang, *Phys. Rev. Lett.* **91**, 078301 (2003).

²⁵M. Xiao, I. Martin, E. Yablonovitch, and H. W. Jiang, *Nature (London)* **430**, 435 (2004).

²⁶J. Smith, C. Berven, M. Wybourne, and S. Goodnick, *Surf. Sci.* **361/362**, 656 (1996).

²⁷P. Yu and M. Cardona, *Fundamentals of Semiconductors* (Springer-Verlag, Berlin, 2003), third edition (revised and enlarged).

²⁸P. Mooney, *J. Appl. Phys.* **67**, R1 (1990).

²⁹P. Mooney, *Semicond. Sci. Technol.* **6**, B1 (1991).

³⁰N. Chand, T. Henderson, J. Klem, W. T. Masselink, R. Fischer, Y.-C. Chang, and H. Morkoç, *Phys. Rev. B* **30**, 4481 (1984).

³¹Although relatively shallow etching (depth ~ 70 nm), an edge depletion effect has to be considered in submicron devices. We find that in our samples the actual feature size (here $0.7 \mu\text{m}$) is about $0.15\text{--}0.2 \mu\text{m}$ smaller than the nominal size determined by lithography and showing in electron micrographs.

³²Y. Li, Ph.D. thesis, Florida State University, 2003.

³³W. Walukiewicz, H. E. Ruda, J. Lagowski, and H. C. Gatos, *Phys. Rev. B* **30**, 4571 (1984).

³⁴R. Petritz, *Phys. Rev.* **110**, 1254 (1958).

³⁵Note that according to $V_H = R_H BI$, where $R_H = 1/ne$ is the Hall coefficient, whether the high or low state corresponds to lower or higher electron concentration of the system, respectively, can only be determined by Hall measurement on a single cross, instead of $\Delta V_H = V_{H1} - V_{H2}$.

³⁶The window of convenient observation times is limited by lock-in response time at one end and experimenter's patience at the other.

- ³⁷ Assuming a somewhat different model following Ref. 9 with an electron capture rate $1/\tau = \sigma \langle v \rangle n$, where σ is the capture cross section, $\langle v \rangle$ the average carrier velocity and n the free carrier concentration, gives $\tau_c \sim T^{-2} \exp(-E_c/k_B T)$ and $\tau_e \sim T^{-2} \exp(-E_e/k_B T)$ for the capture and emission times, respectively, and $E_c = 215$ and $E_e = 160$ meV from the data in Fig. 2. These values are within the error bar similar to those read from Fig. 2(b). The same is true for another model $\tau_c \sim T^{-1/2} \exp(-E_c/k_B T)$ as proposed in Ref. 19.
- ³⁸ N. Casweel, P. Mooney, S. Wright, and P. Solomon, Appl. Phys. Lett. **48**, 1093 (1986).
- ³⁹ The increasing amplitude V_H of the RTS with decreasing gate voltage as seen in Fig. 3(a) is due to the decreasing carrier density; see Fig. 2(b) in Ref. 4. The *relative* change $\Delta V_H/V_H = -\Delta N/N$ remains constant within the experimental error.
- ⁴⁰ The Schrödinger and Poisson equations for the present 1D high electron mobility transistor structure have been solved using the nextnano³ module <http://www.wsi.tum.de/nextnano3>; the band parameters are taken from I. Vurgaftman, J. R. Meyer, and L. R. Ram-Mohan, J. Appl. Phys. **89**, 5815 (2001).
- ⁴¹ K. Hirakawa, H. Sakaki, and J. Yoshino, Appl. Phys. Lett. **45**, 253 (1984).
- ⁴² M. Kirton and M. Uren, Adv. Phys. **38**, 367 (1989).
- ⁴³ K. S. Ralls, W. J. Skocpol, L. D. Jackel, R. E. Howard, L. A. Fetter, R. W. Epworth, and D. M. Tennant, Phys. Rev. Lett. **52**, 228 (1984).